J Mater Sci (2008) 43:3149–3152
DOI 10.1007/s10853-008-2500-x

Electrochemical investigation of silicon/carbon composite as anode material for lithium ion batteries

Pengjian Zuo · Zhenbo Wang · Geping Yin · Dechang Jia · Xinqun Cheng · Chunyu Du · Pengfei Shi

Received: 12 December 2007 / Accepted: 24 January 2008 / Published online: 28 February 2008

Abstract Silicon-graphite composites were prepared by mechanical ball milling for 20 h under argon protection. The microstructure and electrochemical performance of the composites were characterized by X-ray diffraction (XRD), scanning electron microscopy, and electrochemical experiments. XRD showed that the materials prepared by ball milling were composites consisting of Si and graphite powders. The composite electrode showed the best performance, especially when annealed at 200 °C for 2 h, which had a reversible capacity of 595 mAh g^{-1} and an initial coulombic efficiency of 66%, and still retained 469 mAh g^{-1} after 40 cycles with about 0.6% capacity loss per cycle.

Introduction

In recent years, the graphitizating and non-graphitizating carbon materials such as natural graphite, artificial graphite [1], active carbon [2], pitch cokes [3], and carbon fibres [4] were investigated for use as anodes in rechargeable lithium batteries. Moreover, silicon and tin-based materials, which possess high theoretical capacities in comparison with typical graphite anode, have attracted more attention in order to meet the demand for higher energy density power sources for compact portable electronic devices [5–8]. However, the huge volume changes occurring in the lithium alloying and de-alloying process lead to mechanical failure of the metal-based anode material [9–11]. Much effort has been made to overcome this problem for intermetallic electrodes by using composite materials, in which an electrochemically active phase is homogeneously dispersed within an electrochemically inactive matrix [12–14]. In regard to silicon-based anode materials, the Si/C based composites have been reported for anode materials and showed higher reversible capacity with respect to graphite and better capacity retention with respect to pure silicon. Yang et al. [15] reported that silicon and graphite-based composite prepared by pyrolyzing polyvinyl chloride dispersed with nanosized silicon and fine graphite particles showed a reversible capacity $\sim$700 mAh g^{-1} with good cyclability. The carbon-coated nanocomposites were prepared by Nga et al. [16] through spray-pyrolyzing process and the obtained silicon/disordered carbon materials can reveal a high reversible capacity and cycle stability.

In our group, we had succeeded to obtain the Si/Mn/C [17], Si/Cu/C[18], and carbon-coated silicon [19] composites and obtained the satisfied reversible capacity and cycle performance. In order to develop the silicon-based materials for the possible commercialization, the silicon-graphite composite anode material has been prepared by simple mechanical ball milling, and the microstructural analysis and electrochemical performance are also discussed.

Experimental

To fabricate silicon/carbon composites, we used Si powders (purity 99%, 320 mesh Dadi Co., China) after treated

P. Zuo · D. Jia
Postdoctoral Station of Materials Science and Engineering, School of Materials Science and Engineering, Harbin Institute of Technology, Harbin 150001, China

P. Zuo (✉) · Z. Wang · G. Yin · X. Cheng · C. Du · P. Shi
Department of Applied Chemistry, Harbin Institute of Technology, Harbin 150001, China
e-mail: zuopj@hit.edu.cn

by 10 h ball milling and graphite (mean particle size: 18 μm) from Beiruite Co., Shenzhen, China. A mixture of silicon and graphite with a mass ratio of 1:4 was put into a stainless steel vial. The vial was evacuated and then purged with pure argon. The ball milling was carried out in a planetary ball milling machine (ND-6, Nanjing Zuntian Co., China) for 20 h at a rotation speed of 200 rpm. The powders were characterized by X-ray diffraction (XRD) and scanning electron micrograph (SEM). XRD was performed using a D/Max-rB diffractometer equipped with Cu Kα radiation. The particle size and microstructure of electrode materials were observed by SEM (Hitachi S-4700). The sample electrodes after cycling were soaked into DMC and then dried to observe the SEM images.

The electrodes were prepared by drying an electrode slurry (85% of active material, 5% acetylene black, and 10% of PVDF dissolved in *N*-methyl-2-pyrrolidine) on a copper foil at 120 °C for 14 h under vacuum. Cells were assembled in a glove box filled with argon using a lithium foil as a counter and reference electrode. Heat treatment of the electrodes was performed in a tube stove with argon flow at 200 °C. Cyclic voltammograms were conducted in the cell at 0.2 mV s^{-1} using CHI630A. The electrode properties at room temperature were tested by charge–discharge measurements under a constant current density of 0.15 mA cm^{-2} and voltage range from 0.02 to 1.5 V. We regarded Li intercalation to anode as discharge and the opposite as charge.

Results and discussion

Figure 1 shows that the XRD patterns of the silicon-graphite powder composites prepared by mechanical milling. From the figure, we can conclude that the prepared materials are mixtures of silicon and graphite and no new alloy phase occurred during ball milling. Figure 2 shows an image of the silicon-graphite composite electrode, in which the silicon-graphite powders prepared by ball milling was mixed with PVDF and acetylene black homogeneously.

Figure 3 shows the cyclic voltammogram of the silicon-graphite composite electrode consisting of ball milled composite material, PVDF, and acetylene black. It can be indicated that two distinct reductive peaks around 0.4–0.6 V and 0–0.2 V are corresponding to the formation of the SEI film (0.4–0.6 V) and insertion of lithium into silicon and graphite. The reductive peak in regard to the reaction of SEI film formation due to the decomposition of electrolyte does not appear after the first cycle, which indicates that the silicon as anode material for lithium ion battery has the similar reactive process during the first intercalation of lithium into host material in comparison with typical graphite. Figure 4 shows the charge/discharge

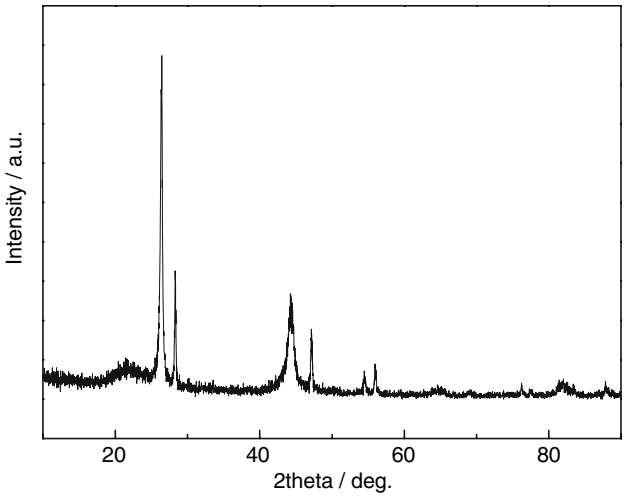

Fig. 1 XRD patterns of silicon-graphite composite powders prepared by 20 h ball milling

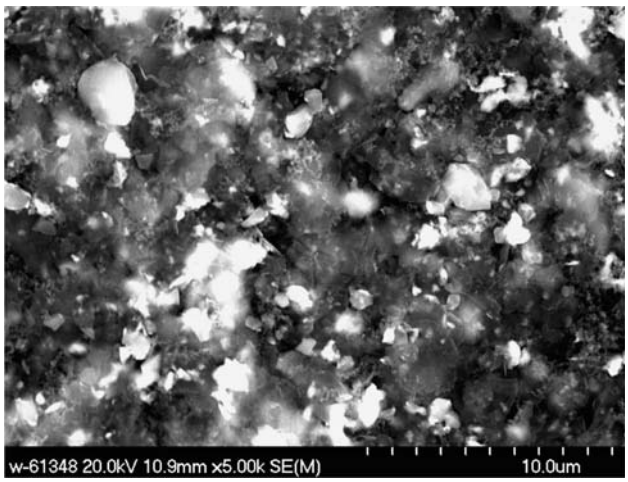

Fig. 2 SEM of silicon-graphite composite electrode prepared by 20 h ball milling

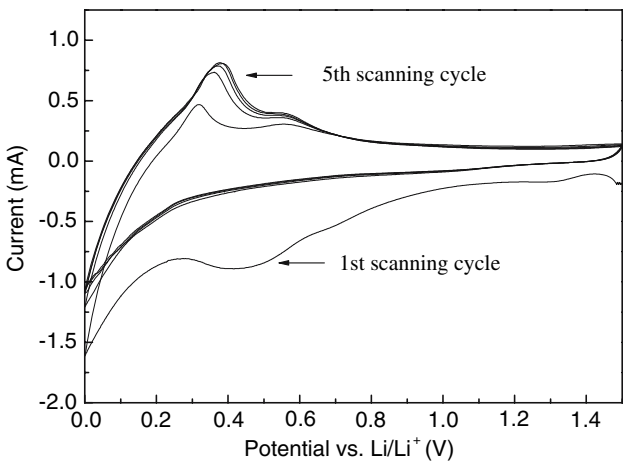

Fig. 3 Cyclic voltammograms of silicon-graphite composite powders prepared by 20 h ball milling

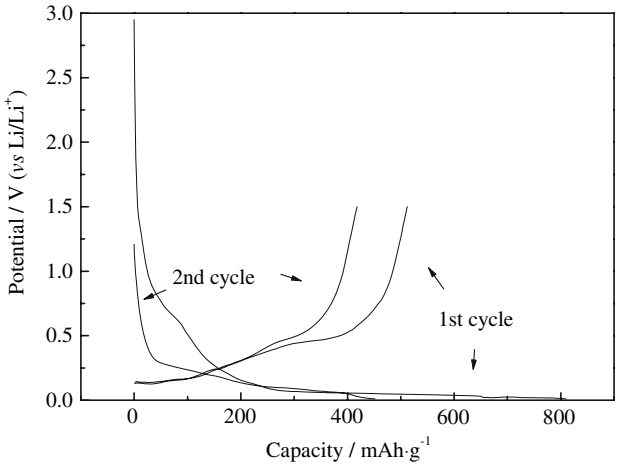

Fig. 4 The charge–discharge curves of silicon-graphite composite powders prepared by 20 h ball milling

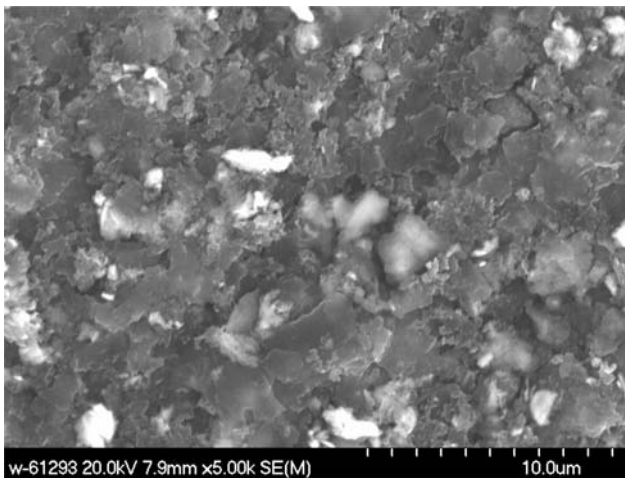

Fig. 6 SEM of silicon-graphite composite electrode after 40 cycles

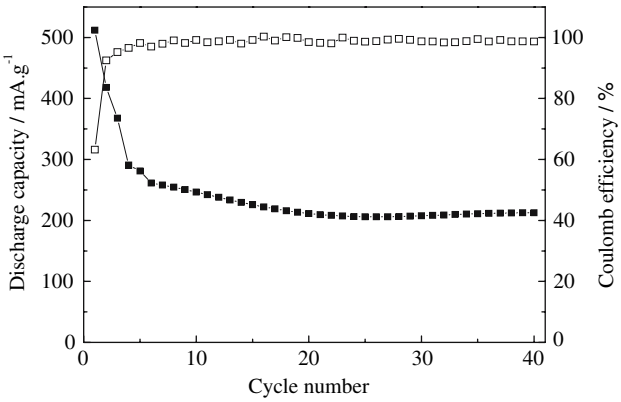

Fig. 5 Discharge capacity and coulomb efficiency versus cycle number for silicon-graphite composite electrode

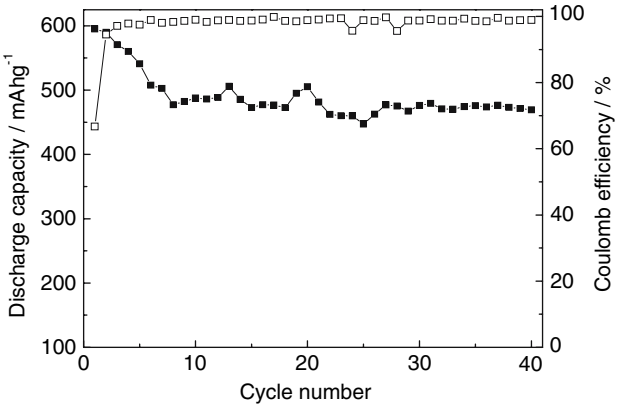

Fig. 7 Discharge capacity and coulomb efficiency versus cycle number for silicon-graphite composite electrode annealed at 200 °C for 2 h

curves of silicon-graphite composite electrode. From the data, it can be seen that the composite electrode has an initial intercalation capacity of over 800 mAh g^{-1}, which significantly exceed the theoretical capacity of 372 mAh g^{-1} for graphite. A voltage platform at about 0.6 V during the first intercalation process corresponds to the decomposition of electrolyte, which is in good agreement with the CV data as shown in Fig. 3.

Figure 5 shows the curves of discharge capacity and coulomb efficiency versus cycle number for silicon-graphite composite. The electrode has an initial reversible capacity of 512 mAh g^{-1} and a coulomb efficiency of 63% which exceed 96% after the third cycle. Its reversible capacity keeps 212 mAh g^{-1} after 40 cycles. It can be found that the irreversible capacity loss is very big during the initial cycles and becomes stable during the 10th cycle. Figure 6 shows the SEM of the silicon-graphite composite electrode after 40 cycles. It can be seen clearly that many dispersed particles coalesce into a big flocculation structure. Based on the morphology variation, this phenomenon can be called electrochemical sintering, which is generally considered as the main source of irreversible capacity loss [8].

The heat treatment of electrode materials can improve the surface morphology and the affinity between the particles and the current collector, which is beneficial to improve the cyclic stability of composite electrode. The reversible capacities curves of the silicon-graphite composites annealed at 200 °C for 2 h are shown in Fig. 7. It is found that the annealed composite exhibits the better capacity property and cycle stability than that of silicon-graphite electrode before heat treatment. Figure 7 shows the curves of discharge capacity and coulomb efficiency versus cycle number for the composite. The electrode annealed at 200 °C has an initial reversible capacity of

595 mAh g^{-1} and a coulomb efficiency of 66%, which exceeds 97% after the third cycle. Its reversible capacity still retains 469 mAh g^{-1} after 40 cycles with about 0.6% loss per cycle, which is better than that of typical graphite. Graphite, which presents little volume changes and possess good cyclic stability during the charge–discharge process, alleviates the huge morphology changes and obviously improves the cycleability of the active material (Si), especially after the heat treatment of composite electrode.

Conclusion

The silicon-graphite composite was synthesized by mechanical ball milling for 20 h. The composite powders show a good cycleability and the cycle performance is improved significantly after the composite electrodes was heated at 200 °C for 2 h under argon. The composite electrode possesses an initial reversible capacity of 595 mAh g^{-1} and an initial coulomb efficiency of 66%. The composite electrode still maintains a high capacity of 469 mAh g^{-1} after 40 cycles with $\sim$0.6% loss per cycle. Silicon-graphite composite is an attractive anode material for new high-energy density lithium ion batteries.

Acknowledgements This work was partially supported by The Natural Science Foundation of China (no. 20673032) and the Key Scientific & Technological Programme of Heilongjiang Province of China (no. GB06A309).

References

1. Fong R, Sacken UV, Dahn JR (1990) J Electrochem Soc 137:2009
2. Yang HX, Ai XP, Lei M, Li SX (1993) J Power Sources 43–44:399
3. Dahn JR, Fong R, Spoon MJ (1990) Phys Rev B 42:6424
4. Endo M, Nakamura JI, Sasabe Y, Takahashi T, Inagaki M (1994) TANSO 165:282
5. Huggins RA (1999) J Power Sources 81–82:13
6. Winter M, Besenhard JO (1999) Electrochim Acta 45:31
7. Beaulieu LY, Hewitt KC, Turner RL, Bonakdarpour A, Abdo AA, Christensen L, Eberman KW, Krause LJ, Dahn JR (2003) J Electrochem Soc 150:A149
8. Li H, Huang X, Chen L, Zhou G, Zhang Z, Yu D, Mo Y, Pei N (2000) Solid State Ionics 135:181
9. Hatchard TD, Topple JM, Fleischauer MD, Dahn JR (2003) Electrochem Solid State Lett 6:A129
10. Obrovac MN, Christensen L (2004) Electrochem Solid-State Lett 7:A93
11. Zuo P, Yin G (2006) J Alloys Compd 414:265
12. Anani A, Huggins RA (1992) J Power Sources 38:363
13. Moriga T, Watanabe K, Tsuji D, Massaki S, Nakabayashi I (2000) J Solid State Chem 153:386
14. Wang GX, Sun L, Bradhurst DH, Zhong S, Dou SX, Liu HK (2000) J Alloys Compd 306:249
15. Yang J, Wang BF, Wang K, Liu Y, Xie JY, Wen ZS (2003) Electrochem Solid State Lett 6:A154
16. Nga SH, Wang J, Konstantinov K, Wexler D, Chew SY, Guo ZP, Liu HK (2007) J Power Sources 174:823
17. Zuo PJ, Yin GP, Zhao J, Ma YL, Cheng XQ, Shi PF, Tamamura T (2006) Electrochim Acta 52:1527
18. Zuo PJ, Yin GP, Hao XF, Yang ZL, Ma YL, Gao ZG (2007) Mater Chem Phys 104:444
19. Zuo PJ, Yin GP, Ma YL (2007) Electrochim Acta 52:4878